Journal of Thermal Analysis and Calorimetry, Vol. 81 (2005) 549–554

EFFICIENT THERMAL CONVERSION OF POLYYNE-TYPE CONJUGATED POLYMERS TO NANO-STRUCTURED POROUS CARBON MATERIALS

M. Kijima[*]*, D. Fujiya, T. Oda and M. Ito*

Institute of Materials Science, Graduate School of Pure and Applied Sciences, University of Tsukuba, 1-1-1 Tennodai, Tsukuba, Ibaraki 305-8573, Japan

Some aromatic based conjugated polymers having carbon–carbon triple bonds moiety were synthesized and carbonized. The polymers were efficiently carbonized by heating up to 900°C under an argon atmosphere, affording porous carbons in high yields. The polymer characteristics were appropriate to form nano-structured carbons in the pyrolytic carbonization process. The carbon materials were consisted of 2–4 nm sized graphitic crystallites and had slit-shaped micropores with ca. 0.7 nm pore width. Structural defects in the pre-carbon materials caused generation of mesopores with ca. 4 nm pore width after carbonization.

Keywords: *conjugated polymers, nano-structure, porous carbon, pyrolysis, TG/DTA*

Introduction

Recently, various nanocarbons classified into nano-sized carbons and nano-structured carbons [1] have been developed since findings of fullerenes and carbon nanotubes. For instance, micro to nano-structured carbon-electrodes for lithium ion battery, electrical double layer capacitor, and fuel cells are very useful materials to answer recent demands for efficient storages and conversions of energy, because regulation of micro to nano-structures in materials is significant to bring out essential functions of material. However, a lot of effort is necessary for practical mass-production of nano-sized carbons. In addition, systematic preparation methods for nano-structured carbons have little been developed. Conventional pyrolytic conversion of polymeric materials to carbon has the merit of preparing carbon materials in an appropriate form in a large mass with simple procedures. Some approaches for synthesis of porous carbons by means of the pyrolytic process have been attempted [2–7]. In general, in order to bring about nano-structures in carbon materials by the pyrolytic carbonization method by design, the polymers having rigid skeletons must be efficiently converted to carbon in a simple mechanism as illustrated in Fig. 1. The polymer materials must uniformly undergo selective elimination or shrinkage, and must have rigid character so as not to be closed the pore spaces during the carbonization process by softening or melting. If unexpected reactions occur during the process, the porosity will fall into disorder.

Some aromatic based π-conjugated polymers such as poly(*p*-phenylene) P*p*P, [8] poly(*p*-phenylenevinylene) P*p*PV, [9] and poly(*m*-phenylenebutadiynylene) P*m*PB [10–12], have been recognized as a good precursor for graphitic carbon materials by pyrolytic carbonization. They all have rigid character with high carbon content over 94%, which seems to be appropriate for the starting material in the thermolytic nano-structuring process. The pyrolyzed P*p*P at 700°C have kept the mesoporosity of P*p*P but the porosity was low [13], while P*p*PV was inappropriate to form porous carbons. Recently, we have reinvestigated the carbonization process of poly(phenylenebutadiyne)s PPBs, finding that the microporous carbonaceous material was produced in high yield (ca. 90%) only by heating up from room temperature to 900°C under an argon atmosphere [14]. Thus the conjugated polymers having carbon-carbon triple bonds moiety are thought to be a potential starting polymer for preparation of nano-structured porous carbons. In this paper, carbonization reactions of some polyyne-type conjugated polymers are investigated focusing on the process of pore formation under the pyrolytic conditions, and nano-structures of the carbonized materials are characterized.

Experimental

Materials and preparations

PPBs (P*m*PB, P*p*PB) were prepared by oxidative condensation of corresponding diethynylbenzene (*m*-, or *p*-) in the presence of CuCl and N, N ,N’,N’-tetramethyl-

---

[*] Author for correspondence: kijima@ims.tsukuba.ac.jp

1388–6150/$20.00

Akadémiai Kiadó, Budapest, Hungary
Springer, Dordrecht, The Netherlands

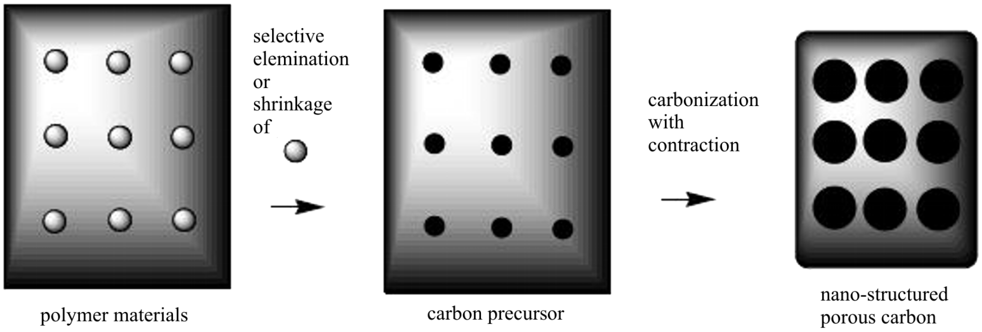

Fig. 1 Image for formation of nano-structures in thermolytic carbonization of polymer materials

ethylenediamine in tetrahydrofuran according to the procedure by Hay [10]. Poly(*p*-phenyleneoctatetraynylene) P*p*PO was prepared by similar procedures [15]. Purification of polymer was carried out by precipitation and washing from MeOH solutions containing aq. HCl, and aq. NH_3, respectively, as described in the previous paper [14] The polymer was dried under vacuum. Diethynylbenzenes (*p*- and *m*-) were purchased from Tokyo Kasei Co. Ltd. Poly(phenylene-ethynylene)s PPEs were prepared from corresponding dibromobenzene (*p*-, or *m*-) and diethynylbenzene (*p*- or *m*-) by Sonogashira coupling using a Pd-Cu catalyst in triethylamine [16]. Solvents were purified by usual manners and other chemicals used in this work are in reagent grade.

The polymer in a form of powder or disk-like pellet (ϕ=13 mm) prepared under a pressure of 4 MPa was carbonized in a quartz tube by heat treatment with a constant heating rate from room temperature to 900°C under an argon atmosphere with a furnace, EKRO-12K (Isuzu). The typical procedure of carbonization was as follows; a polymer disk-pellet sample (30~60 mg) was heated up from room temperature to 300°C at a heating rate of 1°C min^{-1} and from 300 to 900°C at a rate of 10°C min^{-1}, which was allowed to cool down to room temperature after reaching 900°C.

Measurements

Thermal analyses were carried out by an Extra 6000 TG/DTA (Seiko) using a sample (3~5 mg) in a form of powder at a heating rate of 10°C min^{-1} under an argon atmosphere. The powder XRD spectra were measured with a Rint 2100 (Rigaku) with Cu–K$_\alpha$ (1.6418 Å) radiation. Scanning and transmission electron microscope (SEM and TEM) images were acquired with a JSM-5610 and a JEM-2010F (Jeol), respectively. The pore structure of the sample was characterized with N_2 adsorption isotherm at 77 K by using a SA3100 (Coltar).

Results and discussion

General properties of polyyne-type conjugated polymers

The chemical structures of polyyne-type conjugated polymers investigated in this paper are summarized in Fig. 2. PPBs (P*p*PB and P*m*PB) were prepared from corresponding diethynylbenzene by Hay method, whose end group was ethynyl (–C≡C–H), which was confirmend by IR. Molecular terminal of poly(*p*-phenylene-octatetraynylene) P*p*PO similarly prepared was basically butadiynyl (–C≡C–C≡C–H) but the protective triethylsilyl residue remains a little. In the cases of poly(phenyleneethynylene)s PPEs, considerable amount of bromide was remained as the terminal residue, which was confirmed by elemental analysis. A random copolymer consisting of *p*-phenyleneethynylene and *m*-phenyleneethynylene moieties abbreviated as P*pm*PE was prepared from *p*-diethynylbenzene and *m*-dibromobenzene. Poly(2,5-pyridinediylethynediyl) abbreviated as P_{25}PyE was similarly synthesized from 2,5-diethynylpyridine and 2,5-dibromopyridine. These polymers have general characters of rigid molecules consisting of strong bonds and almost insoluble in common organic solvents. Powder X-ray diffraction spectra of these polymers suggest they are crystalline to some extent with chain distances between 0.35–0.50 nm. In order to confirm the

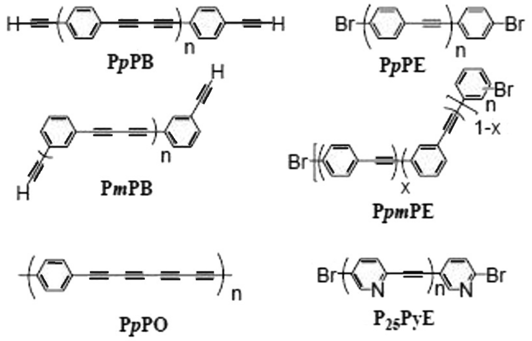

Fig. 2 Chemical structures of polyyne-type conjugated polymers

Table 1 Comparison of bond dissociation energies between sp^3-C–X bonds and sp-, sp^2-C–X bonds in typical organic molecules[a]

sp^3-C–X bonds		sp-, sp^2-C–X bonds	
The broken bonds	BDEs/kJ mol^{-1}	The broken bonds	BDEs/kJ mol^{-1}
CH_3–**H**	439	C_6H_5–**H**	472
		HC≡C–**H**	557
CH_3–$\mathbf{CH_3}$	377	$H_2C\bullet\ \bullet\mathbf{CH_2}$	728
		HC≡**CH**	960
CH_3–**Br**	294	C_6H_5–**Br**	336

[a] Boldface means the dissociated part of molecule. BDEs data are quoted from a book [17]

thermochemical stability of the conjugated polymers, typical bond dissociation energies (BDEs) [17] are compared in Table 1. Wide-used polymeric materials are mainly consisting of sp^3-hybrid C–X bonds, while conjugated polymers are consisting of only sp- or sp^2-C–X bonds, where **X** means C, H, and other atoms. The sp- or sp^2-C based multiple bonds are apparently stronger than the sp^3-C based single bond. BDEs of π-conjugated linkages in an alternate bond system are within those of the multiple bonds and the single bonds, which is dependent on degree of conjugation in the molecule. Thus, it is considered that, intrinsically the polyyne-type conjugated polymers have a good thermal stability.

Investigations of carbonization process

Typical curves of thermogravimetry/differential thermal analysis (TG/DTA) for polyyne-type conjugated polymers are shown in Fig. 3. From TG results, the mass loss at 900°C for P*m*PB was within 10%, but the loss for P*p*PO and P*p*PE were above 20%. DTA results show that P*m*PB has a sharp exothermic peak around 200°C, which is characteristic of PPBs. The shape and the peak temperature of the exothermic reaction depend on chemical structures of PPBs [14, 18]. P*p*PO has a similar exothermic peak, while P*p*PE shows only mild heat flows.

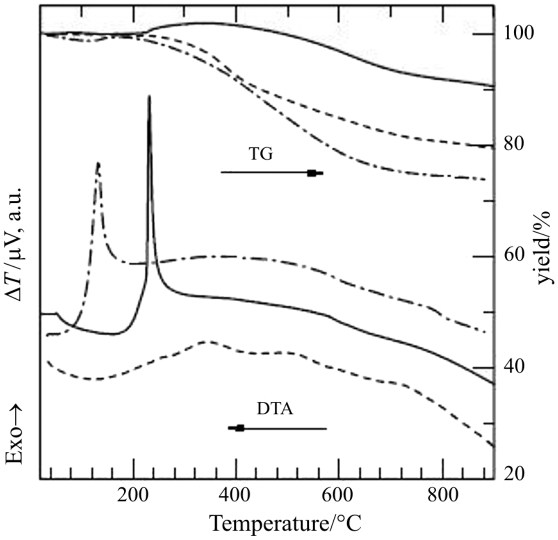

Fig. 3 TG/DTA curves of –– – P*m*PB, - - - – P*p*PO, – · – · – P*p*PE

At first, it is focused on initial thermal reaction around the exothermic peak (<ca. 300°C). It has been well-known that some polyacetylenic compounds (R–(C≡C)$_n$–R) undergo topochemical polymerization, when the acetylenic compounds (n>2) take appropriate configuration in a solid-state [19]. Thus, PPBs and P*p*PO in the solid-state undergo the similar reaction around the exothermic peak, affording a cross-linked polymer. However, the absolute values of heat of reaction (ΔH_{exo}) per molar acetylene unit for PPBs and P*p*PO are almost identical to 30 kJ smaller than those for the topochemical process. The ΔH_{exo} can be estimated by subtracting BDE of C≡C to C=C from total bond energies newly formed by the cross-linking reaction, thus degree of cross-linking reaction affects ΔH_{exo}. This result suggests that the cross-linking reaction partially occurs between polymer chains. The incomplete reaction is confirmed by previous investigations [14]. Contrary to the cases for PPBs and P*p*PO, P*p*PE undergoes mild cross-linking reaction around 200–300°C. From these results, it is found that all polyyne-type polymers partially cross-link utilizing the carbon-carbon triple bond moiety at low temperature region until 300°C in the heating process, affording a polymer network. Since the polymer network is only consisting of sp- and sp^2-carbon linkages, thermal stability of the material retains.

Next step of the carbonization reaction occurs in the range of 300–600°C. Slight increase of mass in the range of 200–400°C for P*m*PB is due to oxidation of the sample by residual oxygen in the analyzer, which means that the cross-linked polymer network material becomes extremely sensitive to O_2. On the other hand, considerable mass loss was observed for P*p*PO and P*p*PE, which is mainly due to elimination of molecular terminal residues. In this stage, fine carbon network consisting of sp^2-carbons with phenylene cores is formed by successive elimination of unstable organic residues, aromatization, and recombination.

The last step of the carbonization occurs above 600°C. Slight decrease of mass in this region is due to elimination of hydrogen. Condensation of aromatic components and construction of graphitic crystallites take place during the last heating process until 900°C. The high-yield carbonization behavior of these polymers is ascribed to formation of the thermal stable intermediates of the cross-linked polymer network and successive carbon network.

Graphitic crystallites of the carbonized samples were confirmed by tunneling electron microscopy (TEM). Dimensions of the crystallite domain perpendicular (L_c) and parallel (L_a) to the basal plane and graphitic interlayer spacing d_{002} are estimated from the XRD spectra of the carbonized samples (Table 2). The L values are estimated from the (002) and (110) diffraction peaks in the XRD spectra according to the Scherrer equation ($L=k\lambda/\beta\cos\theta$), where k is the form factor (1.84 for L_c and 0.94 for L_a), λ is the X-ray wavelength, β is the peak width at half maximum in radians, and θ is the peak Bragg's angle [20]. It is noteworthy that dimensions of graphitic crystallites and d_{002} values are almost same in all cases, and d_{002} is considerably wide by comparison with those for usual graphitic carbons.

Generation of porosity

In order to investigate the generation process of porosity, surface analysis of carbonized samples was carried out by N_2 adsorption method. Adsorption isotherms of the P*m*PB disk-pellet samples heat-treated at 300, 400, 500, 600, and 900°C are shown in Fig. 4. Increase of adsorbed volume (V_{ads}) at low relative pressure (P/P_0) is due to monolayer adsorption and micropore filling of N_2, while those at higher P/P_0 (>ca. 0.5) are due to multilayer adsorption of meso- to macropores accompanying capillary condensation.

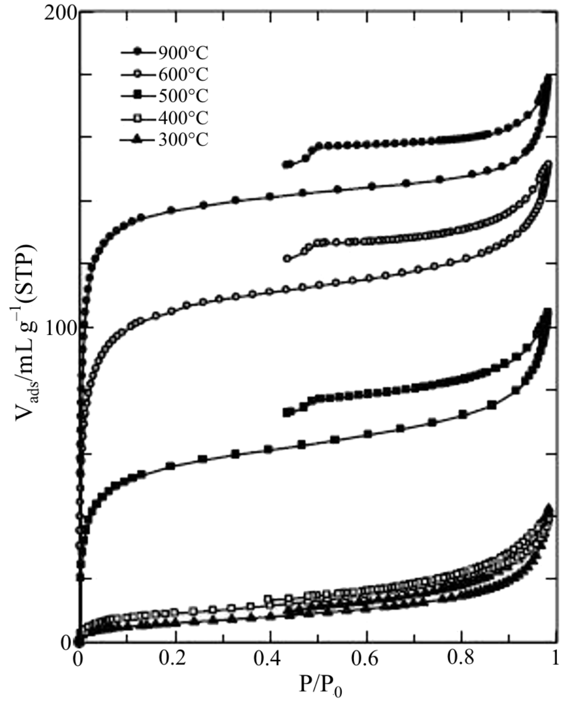

Fig. 4 N_2 adsorption isotherms of the heat-treated P*m*PB samples

The isotherm of P*m*PB heat-treated up to 300°C is classified as type III, suggesting the material is essentially non-porous [21]. The isotherms above 500°C belong to type I but include type IV character, because a gradual increase of V_{ads} in high P/P_0 region and an adsorption-desorption hysteresis are observed, which suggests that materials are microporous but have mesopores in some degree. Adsorbed volume is increased as higher heat-treated temperature. These results suggest that 1) the cross-linked polymer network material has a basis of meso- to macropore structures, 2) formation process of the carbon network brings about basis of microporous structure, and 3) construction of graphitic crystallites promotes the porosity.

Furthermore, correlations of mass decrease, volume contraction, and changes of specific surface area by Brunauer–Emmett–Teller (BET) method (S_{BET}) with heat-treated temperatures of the P*m*PB pellet sample are summarized in Fig. 5. Changes of the parameters can be related to the three steps in the thermolytic carbonization reaction of PPBs, which elucidates generation process of porosity as illustrated in Fig. 6.

In the first step of the thermolytic carbonization, exothermic cross-linking reaction of the conjugated polymers is occurred at the C≡C bond moiety. The starting polymers with uniform structures of alternate phenylene and C≡C bond have a good crystallinity showing close packing of rigid polymer chains (0.35–0.50 nm), which undergoes topochemical-like

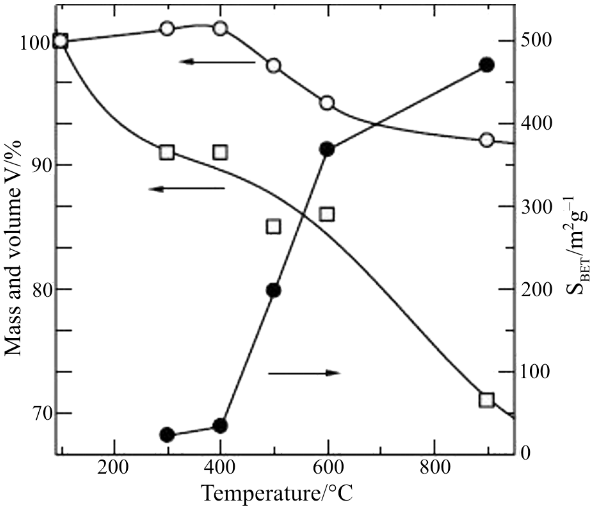

Fig. 5 ○ – Mass, □ – volume, ● – and S_{BET} changes of the heat-treated P*m*PB samples

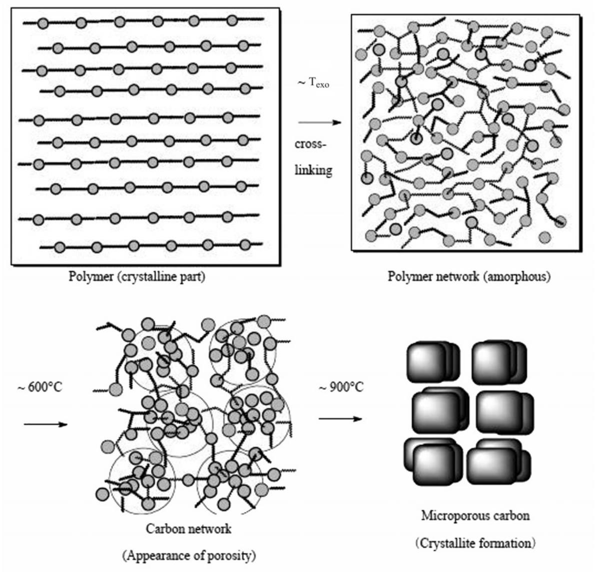

Fig. 6 Schematic formation process of microporous carbon from conjugated polymers having carbon–carbon triple bonds under heating up conditions

partial 1,4- and 1,2-additions, forming the amorphous cross-linked polymer network material. This reaction proceeds without mass loss but accompanying considerable contraction of volume.

In the second step, the fine carbon network is formed. Elimination of unstable organic residues, recombinations, aromatization, and aggregation are occurred at around each phenylene moiety homogeneously dispersed in the material. This step accompanies mass loss but little volume contraction. Accumulation of the phenylene moieties causes generation of inner space but the rigid network frame almost keeps the volume of the material, where basis of microporous structure is determined.

In the last step of the carbonization, hydrogen elimination from aromatic moieties and constructions of graphitic crystallites are occurred. The large contraction of volume is due to formation of crystallites. The gap space between each crystallites corresponds to slit-type micropores of carbon materials. Further heat-treatment of the samples above 1000°C gives rise to decrease of the porosity because of development of crystallites at high temperature, although the carbonized materials from the polymers have hard characters.

Pore structures of carbonized materials

Surface characterization data of some carbonized polymers pyrolized at 900°C are summarized in Table 2 together with crystallographic parameters. Porosity of samples largely depends on pretreatment manners, forms of sample, kinds of polymers, heating conditions and so on. There was no significant difference of porosity (S_{BET}, micropore volume (V_{micro}), micropore width (w) and mesopore volume (V_{meso})) and crystallographic parameters between the carbonized samples prepared from P*p*PB and P*m*PB under same conditions. The porosity develops to some extent, when the sample anneals at 900°C. Exceptionally, the low S_{BET} for P*pm*PE is ascribed to softening (or partial melting) during the carbonization process.

The characterization of micropores was carried out by α_s plot method [22] and the typical plots are shown in Fig. 7. The w of the carbonized materials estimated by the subtracting pore effect (SPE) method is about 0.7 nm. The w for PPEs seems to be smaller than those for PPBs.

Carbonized samples prepared from pellet or powder usually have mesopores to some extent in addition to micropores. The analysis of mesopores is carried out by Dollimore–Heal (DH) method [23]. Distribution curves of mesopore sizes for some carbonized samples suggest that pore radius (R_p) is similar to be about 2 nm (Fig. 8). It is thought that some structural defects in the polymer network or the carbon network develop to mesoporous spacings during the carbonization process. The pore width (about 4 nm) is similar to the sizes of graphitic crystallites. The defects might be induced by disordering of polymer chains, elimination of a leaving group during the carbonization, and so on. A reason for high ratio of V_{meso}/V_{total} for PPEs is that PPEs have bromide residues (about 10 mass %) in the molecular terminal. In fact, the removal of bromine from PPEs brings about decrease the mesoporosity. In contrast, introduction of eliminating moieties into the polymer material must increase the mesoporosity. PPyEs whose typical

Table 2 Carbonization results, structural parameters and surface analysis data

Polymer	Form[a]	Yield/%	V^{b}_{contr}/%	L_a/nm	L_c/nm	d_{002}/nm	S_{BET}/m^2 g^{-1}	V_{micro}/mL g^{-1}	w/nm	V_{meso}/mL g^{-1}
P*p*PB	P	90[c]	18[c]	3.53[c]	2.94[c]	0.39[c]	1019[c]	0.360[c]	0.69[c]	0.202[c]
P*m*PB	P	92	28	2.41	2.65	0.40	470	0.169	0.70	0.057
	P	70[c]	–	–	–	–	1180[c]	0.395[c]	0.70[c]	0.112[c]
	F	89	21	2.16	2.36	0.38	529	0.219	0.71	0
P*p*PE	P	78	15	2.65	2.35	0.40	623	0.222	0.54	0.290
P*pm*PE	P	82	24	2.44	2.40	0.41	71	0.028	0.67	0.015

[a]Form of samples, P – pellet, F – film; [b]Volume contraction; [c]Data of sample annealed at 900°C for 3 h

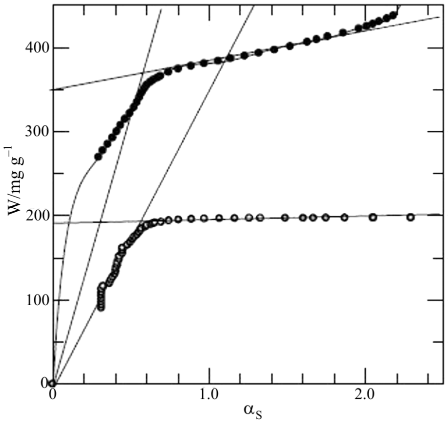

Fig. 7 The α_s plots for carbonized P*m*PB ● – disk and ○ – film samples

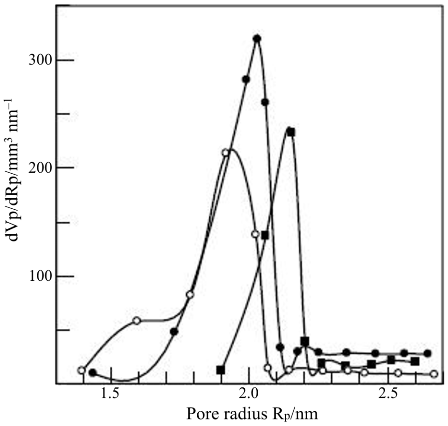

Fig. 8 DH plots for carbonized samples from ● – P*m*PB powder, ○ – P*m*PB pellet, and ■ – P*p*PE pellet

example is shown in Fig. 2 are converted to mesoporous carbons accompanying eliminations of terminal bromide and nitrogen through the carbonization process. For example, the carbonized $P_{25}PyE$ has S_{BET} =422 m^2 g^{-1}, V_{micro}= 0.138 mL g^{-1}, and V_{meso}= 0.395 mL g^{-1}, respectively.

Conclusions

In conclusions, the conjugated polymers having carbon–carbon triple bond moieties were good precursory materials for nano-structured carbons. The polymers were carbonized in high yields by the simple heating up process from room temperature to 900°C under anaerobic conditions. During the carbonization process, rigid polymer materials effectively changed to the cross-linked polymer network below around 300°C, which successively converted to the carbon network materials in the next heating process until around 500°C. In the final step of the carbonization process, the nano-sized graphitic crystallites were selectively formed and the slit-shaped micropores with pore width (ca. 0.7 nm) were generated. On the other hand, presence of defects in the intermediate materials caused formation of mesopores with pore width of ca. 4 nm that was similar size of graphitic crystallites. It is thought that nano-structured carbon materials can be prepared with controlling of crystallite sizes and pore structures by design and further investigations of the thermolytic carbonization method.

Acknowledgements

This work was partially supported by the Grant-in-Aids for the Scientific Research (C) from the Japan Society for the Promotion of Science (No. 15550170), Promotion of Creative Interdisciplinary Materials Science for Novel Functions by The 21st Century COE Program, and University of Tsukuba Research Project. We thank to the Chemical Analysis Center, University of Tsukuba, for NMR spectral, elemental analysis, thermochemical analyses, and surface analyses data.

References

1 M. Inagaki, K. Kaneko and T. Nishizawa, Carbon, 42 (2004) 1401.
2 N. Job, R. Pirard, J. Marien and J. P. Pirard, Carbon, 42 (2004) 619.
3 S. M. Saufi and A. F. Ismail, Carbon, 42 (2004) 241.
4 M. Yamazaki, M. Kayama, K. Ikeda, T. Aii and S. Ichihara, Carbon, 42 (2004) 1641.
5 D. Hines, A. Bagreev and T. J. Bandosz, Langmuir, 20 (2004) 3388.
6 N. Tonanon, A. Siyasukh, W. Tanthapanichakoon, H. Nishihara, S. R. Mukai and H. Tamon, Carbon, 43 (2005) 525.
7 J. M. D. Tascón, J. Therm. Anal. Cal., 79 (2005) 529.
8 E. Fitzer and J. Kalka, High Temp. High Press., 3 (1971) 53.
9 T. Ohnishi, I. Murase, T. Noguchi and M. Hirooka, Synth. Met., 14 (1986) 207.
10 A.S. Hay, J. Org. Chem., 25 (1960) 1275.
11 A. E. Newkirk, A. S. Hay and R. S. McDonald, J. Polym. Sci., Part A, 2 (1964) 2217.
12 J. Economy, H. Jung and T. Gogeva, Carbon, 30 (1992) 81.
13 M. Dubois, A. Naji, J. P. Buisson, B. Humbert, E. Grivei and D. Billaud, Carbon, 38 (2000) 1411.
14 M. Kijima, H. Tanimoto, H. Shirakawa, A. Oya, T. -T. Liang and Y. Yamada, Carbon, 39 (2001) 297.
15 M. Kijima, I. Kinoshita and H. Shirakawa, Chem. Lett., 30 (1999) 531.
16 K. Sanechika, T. Yamamoto and A. Yamamoto, Bull. Chem. Soc. Jpn., 57 (1984) 752.
17 Y.-R. Luo, Handbook of bond dissociation energies in organic compounds, (2003) CRC, Boca Raton.
18 M. Kijima, H. Tanimoto and H. Shirakawa, Synth. Met., 119 (2001) 353.
19 G. Wegner, Makromol. Chem., 154 (1972) 35.
20 T. W. Zerda, W. Xu, H. Yang and M. Grespacher, Rubber Chem. Tech., 71 (1998) 26.
21 S. J. Gregg and K. S. Sing, Adsorption, Surface Area and Porosity, (1982) Academic Press, London.
22 K. Kaneko, C. Ishii, M. Ruike and H. Kuwabara, Carbon, 30 (1992) 1075.
23 D. Dollimore and G. R. Heal, J. Appl. Chem., 14 (1964) 109.

DOI: 10.1007/s10973-005-7079-8